Journal of
Instrumentation

PAPER • OPEN ACCESS

HASPIDE: a project for the development of hydrogenated amorphous silicon radiation sensors on a flexible substrate

To cite this article: L. Tosti *et al* 2024 *JINST* **19** C04025

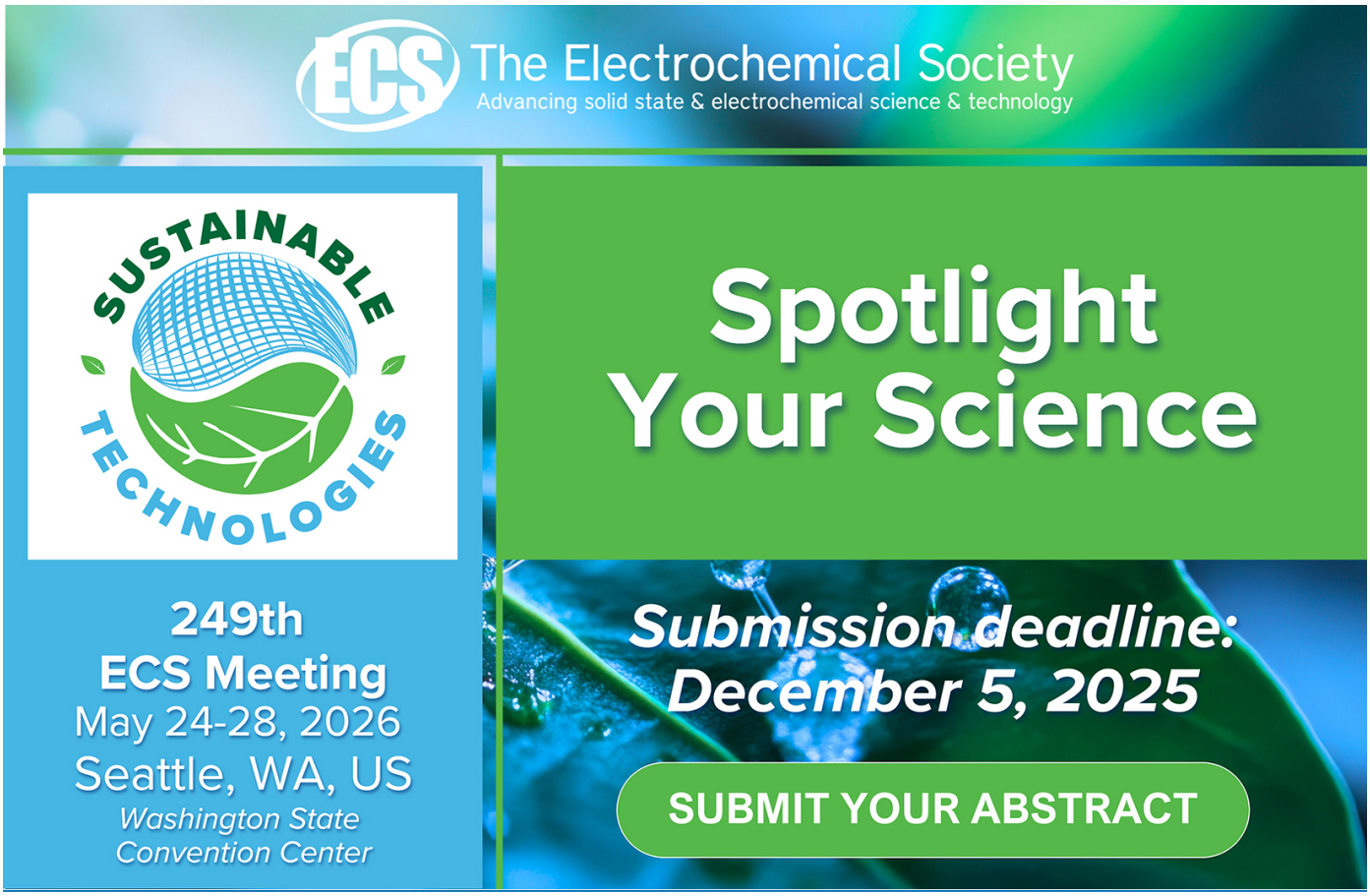

Published by IOP Publishing for Sissa Medialab

Received: *December 11, 2023*
Accepted: *February 17, 2024*
Published: *April 10, 2024*

16TH Topical Seminar on Innovative Particle and Radiation Detectors
Siena, Italy
25–29 September 2023

HASPIDE: a project for the development of hydrogenated amorphous silicon radiation sensors on a flexible substrate

L. Tosti,[a,*] **L. Antognini,**[q] **S. Aziz,**[i,j] **A. Bashiri,**[r,s] **L. Calcagnile,**[i,j] **D. Caputo,**[m,n] **A.P. Caricato,**[i,j] **R. Catalano,**[k] **G. De Cesare,**[m,n] **D. Chilà,**[f,g] **G.A.P. Cirrone,**[k] **T. Croci,**[a,d] **G. Cuttone,**[k] **S. Dunand,**[q] **M. Fabi,**[f,h] **L. Frontini,**[l] **C. Grimani,**[f,h] **M. Ionica,**[a] **K. Kanxheri,**[a,b] **M. Large,**[r] **V. Liberali,**[l] **N. Lovecchio,**[m,n] **M. Martino,**[i,j] **G. Maruccio,**[i,j] **G. Mazza,**[p] **M. Menichelli,**[a,*] **A.G. Monteduro,**[i,j] **A. Morozzi,**[a] **F. Moscatelli,**[a,c] **A. Nascetti,**[m,o] **S. Pallotta,**[f,g] **D. Passeri,**[a,d] **M. Pedio,**[a,c] **M. Petasecca,**[r] **G. Petringa,**[k] **F. Peverini,**[a,b] **L. Piccolo,**[p] **P. Placidi,**[a,d] **G. Quarta,**[i,j] **S. Rizzato,**[i,j] **F. Sabbatini,**[f,h] **L. Servoli,**[a] **A. Stabile,**[l] **C. Talamonti,**[f,g] **J.E. Thomet,**[q] **M. Villani,**[f,h] **R.J. Wheadon,**[p] **N. Wyrsch**[q] **and N. Zema**[a,e]

[a] *INFN, Sezione di Perugia,via Pascoli s.n.c., 06123 Perugia, Italy*
[b] *Dipartimento di Fisica e Geologia, via Pascoli s.n.c., 06123 Perugia, Italy*
[c] *CNR-IOM, via Pascoli s.n.c. 06123 Perugia, Italy*
[d] *Dipartimento di Ingegneria dell'Università degli studi di Perugia, via G. Duranti 06125 Perugia, Italy*
[e] *CNR Istituto struttura della Materia, Via Fosso del Cavaliere 100, Roma, Italy*
[f] *INFN Sezione di Firenze, Via Sansone 1, 50019 Sesto Fiorentino, Firenze, Italy*
[g] *Dipartimento di Scienze Biomediche sperimentali e Cliniche "Mario Serio", University of Florence, Largo Brambilla 3, 50139 Firenze, Italy*
[h] *DiSPeA, Università di Urbino Carlo Bo, 61029 Urbino (PU), Italy*
[i] *INFN Sezione di Lecce via per Arnesano, 73100 Lecce, Italy*
[j] *Department of Mathematics and Physics "Ennio de Giorgi" University of Salento, via per Arnesano, 73100 Lecce, Italy*
[k] *INFN Laboratori Nazionali del Sud, Via S.Sofia 62, 95123 Catania, Italy*
[l] *INFN Sezione di Milano Via Celoria 16, 20133 Milano, Italy*
[m] *INFN Sezione di Roma 1, Piazzale Aldo Moro 2, Roma, Italy*
[n] *Dipartimento Ingegneria dell'Informazione, Elettronica e Telecomunicazioni, Università degli studi di Roma, via Eudossiana, 18 00184 Roma, Italy*
[o] *Scuola di Ingegneria Aerospaziale Università degli studi di Roma, Via Salaria 851/881, 00138 Roma, Italy*
[p] *INFN Sezione di Torino Via Pietro Giuria, 1 10125 Torino, Italy*

[*] Corresponding author.

https://doi.org/10.1088/1748-0221/19/04/C04025

2024 JINST 19 C04025

[q] *Ecole Polytechnique Fédérale de Lausanne (EPFL), Photovoltaics and Thin-Film Electronics Laboratory (PV-Lab), Rue de la Maladière 71b, 2000 Neuchâtel, Switzerland*
[r] *Centre for Medical Radiation Physics, University of Wollongong, Northfields Ave Wollongong NSW 2522, Australia*
[s] *Najran University, King Abdulaziz Rd, Najran, Saudi Arabia*

E-mail: luca.tosti@pg.infn.it, mauro.menichelli@pg.infn.it

Abstract: Hydrogenated amorphous silicon (a-Si:H) is a material with a very good radiation hardness and with the possibility of deposition on flexible substrates like Polyimide (PI). Exploiting these properties, the HASPIDE (Hydrogenated Amorphous Silicon PIxels DEtectors) project has the goal of developing a-Si:H detectors on flexible substrates for beam dosimetry and profile monitoring, neutron detection and space experiments. The detectors for this experiment will be developed in two different structures: the n-i-p diode structure, which has been used up to now for the construction of the planar a-Si:H detectors, and the recently developed charge selective contact structure. In the latter the doped layers (n or p) are replaced with charge selective materials namely electron-selective conductive metal-oxides (TiO_2 or Al:ZnO) and hole-selective conductive metal oxides (MoO_x). In this paper preliminary data on the capabilities of these detectors to measure X-ray and electron fluxes will be presented. In particular, the linearity, the sensitivity, the stability and dark current in various conditions will be discussed.

Keywords: Radiation monitoring; Radiation-hard detectors

2024 JINST 19 C04025

Contents

2024 JINST 19 C04025

1 Introduction

Hydrogenated amorphous silicon (a-Si:H) is a form of amorphous silicon obtained form the addition of hydrogen atoms in an amorphous silicon structure. This fabrication process improves the electrical characteristics of this material used as radiation detector.

Unlike the more commonly used crystalline silicon, a-Si:H inherits from amorphous silicon the characteristic of not having an ordered atomic structure but instead displaying a disordered arrangement of atoms. Hydrogen is introduced into the material to saturate the so-called "dangling bonds" or unpaired bonds that occur in the disordered structure of amorphous silicon. These dangling bonds can cause defects and charge traps in the material, reducing the charge collection efficiency for this material used as radiation sensor.

The hydrogenation reduces the density of defects in the material, improving its structural quality. Furthermore, hydrogen helps regulating the width of the band-gap of amorphous silicon. Another peculiar property of this type of material is the high radiation resistance.

These attributes makes a-Si:H a useful material in various applications, including solar cells, radiation detectors, and electronic devices [1].

One of the most commonly employed techniques for fabricating thin film a-Si:H is plasma-enhanced chemical vapor deposition (PECVD). In order to achieve the proper hydrogen content, the film is grown from a mixture of Silane (SiH4) and hydrogen at temperatures ranging from 250 to 300°C. Due to the low deposition temperature of a-Si:H, it can be easily deposited on plastic materials. This allows the sensor to exhibit strong adaptability to curved surfaces and notable flexibility [2].

The plastic materials most frequently used are based on Polyimide (PI) like Kapton. This material also has the advantage of being considered tissue-equivalent (TEM) [3], and in addition to its high chemical stability and radiation hardness, it allows for use in medical and dosimetric applications.

The HASPIDE project [4] focuses on developing a-Si:H sensors deposited on PI. The envisioned applications include beam monitoring for high-energy physics and TRansmission Detectors (TRD) for electron and proton clinical accelerators, X-ray beam dose profiling for medical and industrial purposes, detectors for solar flare events in space missions [5], and neutron detection for industrial, nuclear safeguard, and homeland security applications [4].

2 Sensors and setup description

The radiation sensors within the HASPIDE project are available in two distinct configurations: n-i-p diodes and charge-selective contact devices (CSC). N-i-p diodes consist of a thin layer (tens of nm) of p-doped a-Si:H, a thicker layer (1–10 µm) of intrinsic a-Si:H, and a thin layer of n-type doped a-Si:H.

On the other hand, charge-selective contact devices [6] follow a three-layer structure, including a thin layer of metal oxides where hole mobility exceeds electron mobility (MoO_x or WO), a thick layer of intrinsic a-Si:H, and a thin layer of a metal oxide where electron mobility is greater than hole mobility (such as TiO_2 or Aluminum-doped Zinc Oxide).

The electric contact of the sensors is provided by a layer of ITO (Indium Tin Oxide) deposited by sputtering.

The sensors used for the characterization described in this paper include 6 pads, differing in their active area: one with 5×5 mm^2 surface and five surrounding pads having 2×2 mm^2 surface. The thickness of the sensors described in this work are 2.5 µm or 5 µm depending on the tested production batch.

Sensors deposited on Kapton are fixed to a dedicated PCB, onto which bonds for the electrical contacts of the sensor will then added.

As illustrated in figure 1, it can be noted that the sensors are positioned within a dedicated opening within the PCB, on an additional layer of Kapton (which serves as support).

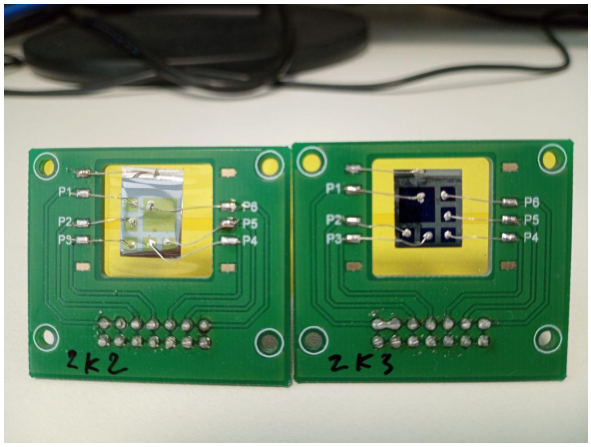

Figure 1. Example of two sample sensors (N-i-p on the left and CSC on the right) mounted on PCB.

This configuration not only allows for complete electrical isolation of the sensor but also provides a minimal material layer for possible dosimetry measurements behind the sensor. The Kapton tape, in fact, can be considered almost transparent and also "tissue-equivalent" for the X-ray spectrum used in these measurements. Its effect can thus be easily identified (and removed if necessary) during the analysis.

The bonds ensuring the electrical contact of the readout pads are soldered with tin soldering on the PCB and with silver-based glue on the sensor under test. The use of glue is necessary as ultrasonic soldering on a-Si:H is not advisable due to adherence problems on the ITO layer.

The various contacts are then grouped in a dedicated connector, one for each pad to be measured. The bias is provided to the pad while the common contact on the sensor film base (composed of n doped a-Si:H or TiO_2) is grounded.

2024 JINST 19 C04025

The measurement setup includes a PCB board for the connection to SMU (Source Measuring Unit, Keithley 2410) that is used also as mechanical support. This assembly is located inside a climatic chamber designed to maintain stable temperature conditions. The radiation source is a X-ray tube (Newton Scientific XRSource 50 KV 10 W and a Semat 200 KV) or a ^{90}Sr electron source.

For the measurements presented, each data acquisition run has been divided into 2 steps. The first step involves IV characterization to obtain preliminary information about the dark current. This helps in selecting the correct bias voltage. The second step is essentially the characterization of the sensor's performance when irradiated by selected dose rates (X-ray radiation) or known electron flux from ^{90}Sr (31 KBq).

It is important to note that the measurements are conducted while keeping the sensor's position fixed, even during dark current measurement. This is done to ensure that X-ray characterization (or with other sources) is performed at a defined and consistently fixed distance (the setup is shown in figure 2a); figure 2b shows the calibration curve dose-rate in function of the tube current.

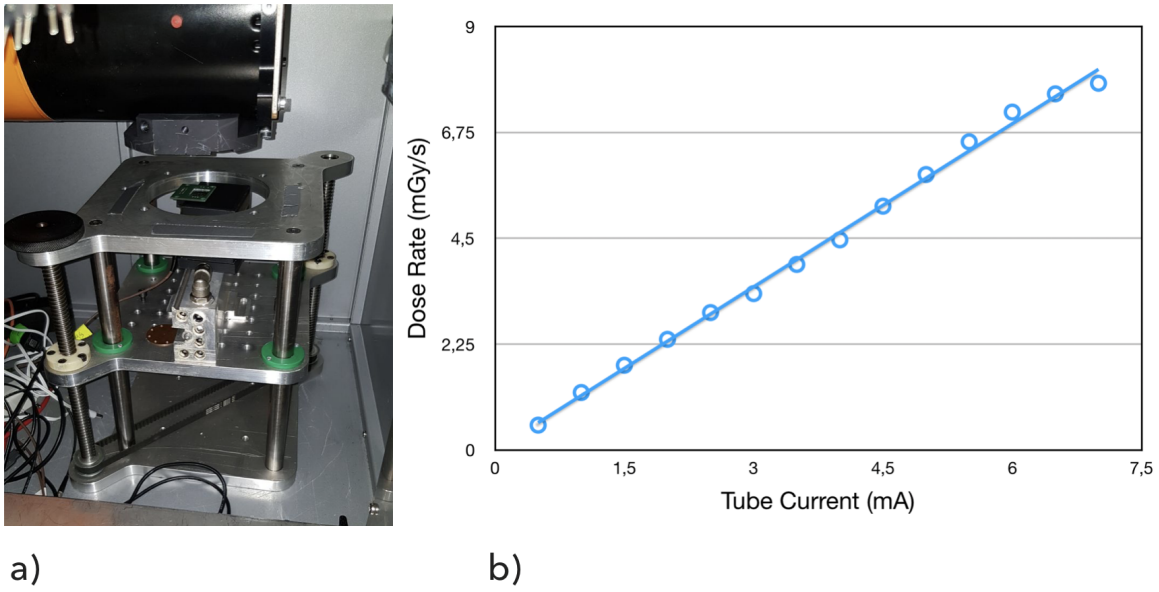

Figure 2. a) Setup installed under the X-ray tube. b) Calibration curve dose-rate as a function of the tube current.

Due to the long time-scale for a-Si:H electrical stabilization, it was necessary to set an initial stabilization time of 600 s for both IV measurements and characterizations with sources.

For the same reason, an additional stabilization time of 180 s was added into the measurement procedure at each voltage change.

The X-ray irradiation is performed at fixed voltage, and consequently, no additional stabilization was foreseen, unlike in the case of IV measurements. Both stabilization times were defined empirically and iteratively to achieve a stable dark current condition considered acceptable.

3 The measurements process

As previously explained, the sensors must undergo an IV characterization session to determine their correct operating voltage and identify any damage due to production defects or handling. In figure 3,

2024 JINST 19 C04025

an example of the IV characterization of two sample sensors from the entire tested population is shown. As observed, the sensors generally exhibit high homogeneity in current measurement, given that they come from the same production batch. This enables the straightforward and relatively quick identification of faulty sensors within the tested population.

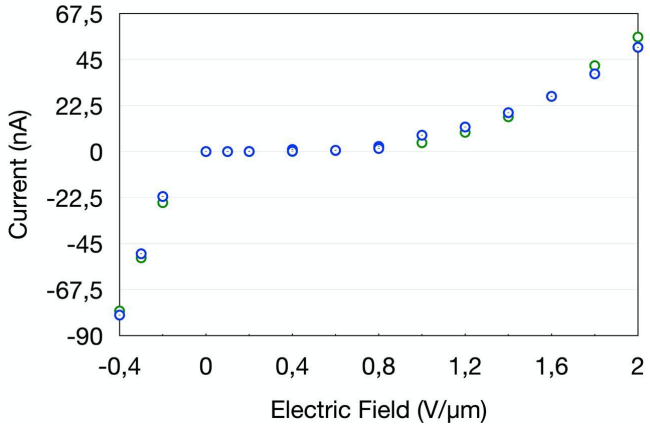

Figure 3. Example of IV characterization for two 5 µm thickness sensors.

In this case, the characterization procedure involves applying a maximum of 2 V/µm in reverse polarization (−5 V). To verify the rectifying properties of the sensors the IV measurement extended to 0.4 V/µm in direct polarization (1 V). It was decided not to exceed this value as higher forward polarization that could risk the damage of the sensor. The maximum expected current in reverse polarization is approximately 60 nA.

The current increase above 0.8 V/µm (−2 V) helps locating the working point at which the sensor is used during most tests.

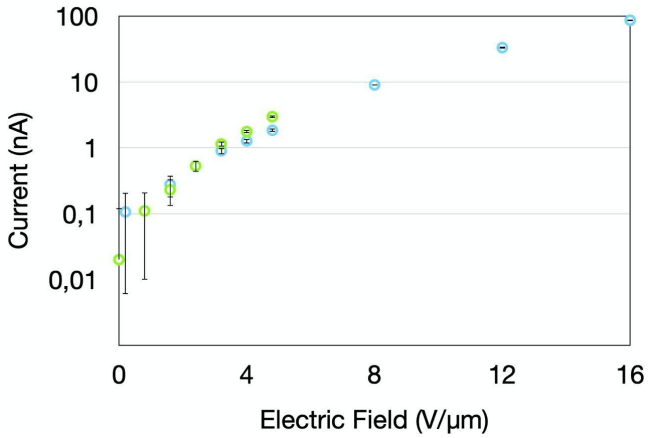

Figure 4. Example of IV characterization for two sensors (2.5 µm of thickness). The first one (in blue) up to 5 V/µm, and the second one (green) up to 16 V/µm.

For some samples (2.5 µm thick sensors), an additional measurement was conducted at voltages up to 16 V/µm (−40 V). This type of measurement was carried out to assess the voltage range in which the sensor can be considered in a saturation condition. In figure 4, it can be seen that even after applying 16 V/µm, the sensors still do not exceed the current value of 100 nA.

2024 JINST 19 C04025

After the IV characterization the performance of the sensors was evaluated under X-ray irradiation and ^{90}Sr electron flux.

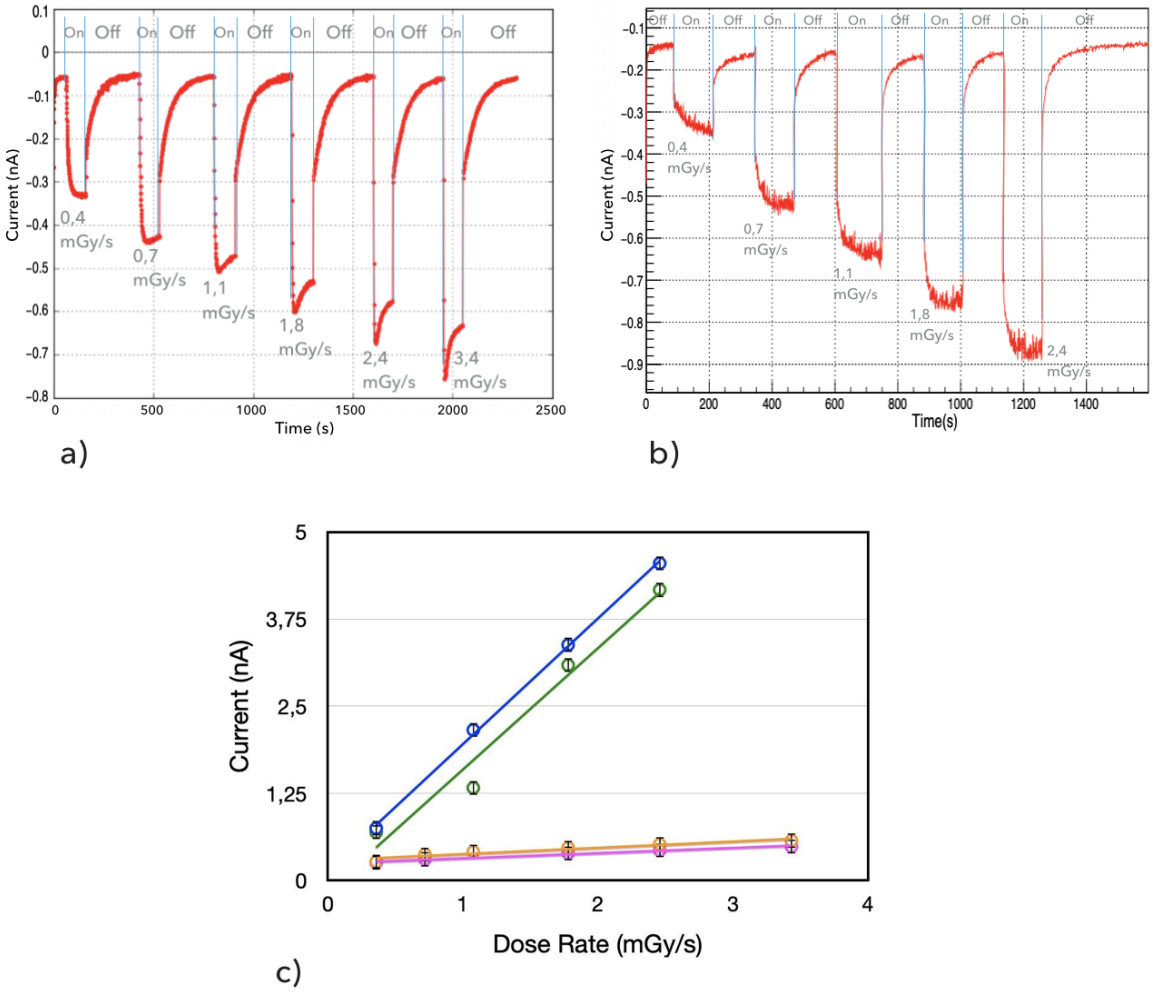

Figure 5. Example of X-ray characterization of a sensor. Figure a) shows real-time data acquisition of the sensor signal at various X-ray dose rates. The sensor was not subjected to annealing. In figure b) the same real-time data acquisition was repeated after an annealing session. The X-ray source activation is sequenced (On-Off in the graph) to optimize dead times due to the electrical stabilization of the sensor. In figure c), the sensitivity of a selected group of sensors before and after the annealing procedure is illustrated.

In figure 5, the characterization of a sensor under X-ray exposure is presented. As evident, the sensitivity maintains linearity with the X-ray dose rate to which the sensor is irradiated. This behavior persists even under intense exposition to light prior to the measurement, but in this case a reduction in the slope is observed due to the effect of light exposure. It has been observed that the sensors can recover their maximum sensitivity after a 12-hour annealing session at 100°C. This consistent behavior across various production batches led to the decision to implement a preliminary annealing session before each characterization session. The annealing procedure also helps to shorten the stabilization time of the signal as it can be observed in figure 5a and figure 5b.

After each measurement, the sensors are stored in individual specialized black boxes to prevent potential damage from light exposure or handling.

2024 JINST 19 C04025

In figure 6, the current generated by the radiation from the ^{90}Sr source, with the contribution due to the dark current subtracted, is presented.

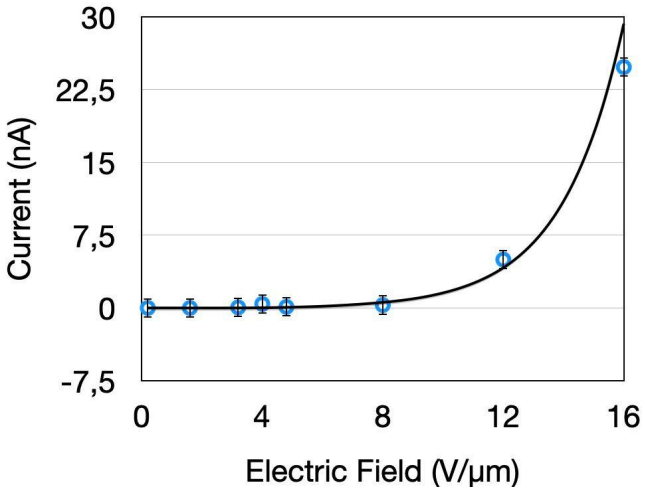

Figure 6. Exponential trend of the sensor signal (electron from ^{90}Sr) as a function of the applied electric field. The dark current was already subtracted from the signal.

Up to approximately 8 V/µm, there is minimal difference between the signal in irradiation condition and the dark current value. However, above 8 V/µm, an exponential trend is observable, suggesting the presence of a charge amplification process. The cause of the signal amplification may be attributed to an avalanche-like effect. The phenomenon is somehow unexpected, and the results are still preliminary. More in-depth studies will be conducted to clarify the presence of an avalanche-like effect.

4 Conclusion

The assembly procedures, electrical characterization of the HASPIDE sensors prototype have been presented. Additionally, measurements were conducted to characterize the sensor performance under X-ray radiation and electrons from a ^{90}Sr source. It was observed that the responses of the detectors to irradiation at different X-ray fluxes is linear in the range of the observations. Leakage current measurements were also performed and subtracted to the observed photocurrent. Effects from annealing on light exposed detectors were also shown demonstrating a substantial increment in sensitivity. Results from the irradiation with ^{90}Sr source at various bias voltages has been shown. The data exhibit an exponential increase of the signal with voltage possibly due to an internal amplification mechanism to be further investigated.

Acknowledgments

The HASPIDE project is funded by INFN through the CSN5 and was partially supported by the "Fondazione Cassa di Risparmio di Perugia" RISAI project n. 2019.0245.

F. Peverini has a PhD scholarship funded by the PON program. M.J. Large is supported by the Australian Government Research Training Program (AGRTP) scholarship and the Australian Institute of Nuclear Science (AINSE) Post-Graduate Research Award (PGRA).

2024 JINST 19 C04025

References

[1] M. Menichelli, L. Servoli and N. Wyrsch, *Status and perspectives of hydrogenated amorphous silicon detectors for MIP detection and beam flux measurements*, *Front. Phys.* **10** (2022) 943306.

[2] M. Menichelli et al., *Characterization of hydrogenated amorphous silicon sensors on polyimide flexible substrate*, arXiv:2310.00495.

[3] I. Amini, P. Akhlaghi and P. Sarbakhsh, *Construction and verification of a physical chest phantom from suitable tissue equivalent materials for computed tomography examinations*, *Radiat. Phys. Chem.* **150** (2018) 51.

[4] M. Menichelli et al., *Development of thin hydrogenated amorphous silicon detectors on a flexible substrate*, arXiv:2211.17114.

[5] C. Grimani et al., *A hydrogenated amorphous silicon detector for Space Weather applications*, *Astrophys. Space Sci.* **368** (2023) 78 [arXiv:2302.00339].

[6] D. Totani and F. Cavanna, *First Calorimetric Energy Reconstruction of Beam Events with ARAPUCA Light Detector in ProtoDUNE-SP*, 2020 *JINST* **15** C03033.

2024 JINST 19 C04025